IOSR Journal of Applied Physics (IOSR-JAP)
e-ISSN: 2278-4861.Volume 10, Issue 4 Ver. II (Jul. – Aug. 2018), 57-71
www.iosrjournals.org

Light Velocity Quantization and Harmonic Spectral Analysis

Javier Joglar Alcubilla
Avionics Department, Barajas College, Spain
Corresponding Author: Javier Joglar Alcubilla

Abstract: *The quantization hypothesis of propagation velocity of any interaction in quantization intervals of size c will allow the generalization of Einstein's relativity principle establishing that "the laws of nature are the same in any inertial reference system, regardless of its application speed coordinate". For its justification we will use the Lorentz transformations of m_degree, supported by a detailed wave equation study with which it is concluded that "the wave propagation speed measured in a given observation does not depend on the origin of the wave, but precisely of the speed coordinate from where the measurement is made". Through spectral analysis, power discrepancies will be observed between generated signals and the equivalent measured signals which are explained through the quantization hypothesis of the propagation velocities of the different harmonics that compose such electromagnetic signals.*

Keywords – *Lorentz transformations, Special relativity, Spectral analysis, Superluminal, Velocity quantization.*

Date of Submission: 02-08-2018 Date of acceptance: 18-08-2018

I. Introduction

The speed of light (*c*), constant and invariable, is the basis of Special Relativity Theory (SR) principles [1]. It is considered in these terms by the results obtained experimentally. Moreover, in Maxwell's equations a characteristic velocity intervenes, the propagation velocity of electromagnetic waves in vacuum, which is also *c* [2]; for this reason, Maxwell's equations are not invariant with respect to the Galileo transformations (GT). To solve it, the SR introduced two basic postulates [3]:

1. Einstein's relativity principle (ERP), whereby "*all the laws of nature are the same in any inertial reference system*" [4]. That is, the laws of nature are invariant when passing from an inertial system to another also inertial. The ERP is a generalization of the Galileo's relativity principle (GRP) [5], though this second is not applicable to the Maxwell's equations, so from these equations the ERP is necessary.
2. The existence principle of an interactions limit propagation velocity, in a vacuum, *c*. With electrodynamics the existence of a finite propagation velocity in electromagnetic interactions is established, which subsequently extends to the other interactions, gravitational, nuclear and weak. The existence of a limit propagation velocity in interactions means that there is a certain relationship between the intervals of space and time, revealed by the SR. It also presupposes a speed limitation of material bodies [6].

We will use the formalism of the Lorentz transformations (LT) for the analysis of the wave equation that relates wavelength, frequency and propagation velocity, under the point of view of the extended relativity (ER) proposed by [7]. Thus, it explains why an inertial observer always interprets the interactions seen in a vacuum with propagation velocity *c*, although they may be propagating at different speeds, in all cases positive integer proportional to *c*, that is, with *mc* (*m=1, 2, …*). In the theoretical development of the ER, quantization hypothesis of propagation velocity of any interaction is introduced in quantization intervals of size *c*, so that it is considered that the interactions can be traveling with velocities *c*, *2c*, *3c*, *..*, *(m + 1) c*, with *m* a positive integer number, naming each of these velocities as speed *0,1, 2, .., m*_coordinates, respectively. Thus, we are able to generalize the LT of the SR [8] in some equations that will serve as generic transformations of movement in any speed m_coordinate, that is, the LT for the speed m_coordinate (LTm) is developed.

The ERP embodied in the LT used by the SR provides invariance in the Maxwell's equations, although at the expense of a constant propagation speed of the electromagnetic interactions. For the ER, the relativity principle that has passed from the GRP to the ERP, is further generalized stating that "*all the laws of nature are the same in any inertial reference system, independently of its speed coordinate of application*", justified from the LTm of the ER, which allows quantization of velocities propagation in electromagnetic interactions.

In the first place, a theoretical application of the above will be developed, checking the compatibility between the LTm equations in the ER, compared with that of the LT equations in the SR [9]. Lorentz transformations of m_degree (LTm) defined in the ER, offers solutions of space and time relative to the velocity of the physical entity observed, a function in turn of the speed coordinate in which it moves. Thus, it can be verified that the LTm is a generalization of the LT used in the SR and, while the LT can only work in the speed

0_coordinate, with the LTm observers and physical entities observed in any generic speed coordinate are admitted. It is going to be shown that the LTm represents a formal justification of the quantization hypothesis of the light speed, compared to the constancy of *c* supported by the LT of the SR.

But, can you theoretically justify the use of the quantization hypothesis of the light speed? It is possible using the search analogy of the wave equation, where the wave propagation speed appears implicit which, traditionally, for any observer in any circumstance is *c* [10]. In this analogy, the ER from the LTm incorporates modifications to the wave equation that allow its generalization, using observers from any speed m_coordinate. The result is that the wave propagation velocity measured in a given observation does not depend on the origin of the wave, but precisely on the speed coordinate from which the measurement is made. That is, a wave emitted from the speed m_coordinate with *(m+1)c* velocity, will be seen with this same velocity as long as the observer belongs to the same speed m_coordinate.

Is it possible experimentally to observe the velocity quantization of an electromagnetic wave? Yes, it will be possible. Two experiments with electromagnetic waves of different shapes (sinusoidal and square) and different frequency ranges will be developed, performing spectral analyzes [11, 12] that will provide us data compatible with the previous statement. That is, the spectral analysis of the waves harmonics used [13] will be compatible with the quantization theory of the speed of light, which represents a real test of its validity.

II. Compatibility Of The Lorentz Transformations For The Speed M_Coordinate

It is intended to find the degree of compatibility between the Lorentz transformations equations in the speed m_coordinate (LTm) developed in the ER, with respect to the one that exists in the LT equations in the SR. To do this, two experiments are presented, one based on SR and the other with the principles of ER, comparing results.

Supposed two observers *O(x,t)* and *O'(x',t')* both moving in the speed 0_coordinate, with relative velocity $v < c$ in the direction *x, x'*. If *O* emits light in the direction *x, x'*, what speed does this light propagate for *O* and *O'* with?

If we have for *O*,

$$x = ct \tag{1}$$

That is,

$$t = \frac{x}{c} \tag{2}$$

And for *O'*,

$$c't' = x' \tag{3}$$

If we use the descriptive equation of time, according to LT in the SR, multiplying by the parameter *c*, we obtain,

$$ct' = \left(ct - \frac{vx}{c}\right)\gamma_0 \text{, with } \gamma_0 = \left[1 - \frac{v^2}{c^2}\right]^{-1/2} \tag{4}$$

Where γ_0 is the Lorentz factor in the speed 0_coordinate.

Introducing (1) and (2) in (4),

$$ct' = (x - vt)\gamma_0 \tag{5}$$

So, using the descriptive equation of position, according to LT in the SR, in (5) we obtain,

$$ct' = x' \tag{6}$$

And, definitely, comparing (3) with (6), we get,

$$c' = c \tag{7}$$

In principle, it could be thought that the previous demonstration serves as a justification that *c* is the same and constant for all inertial observers, using LT according to SR. However, let's see what happens if an analogous experiment is used, but more generic through the ER.

Assumed now two observers *O(x,t)* and *O'(x',t')* both moving on the speed 0_coordinate and the speed m_coordinate, respectively, such that the relative velocity between them is *v* in the direction *x, x'*, being $mc \leq v < (m+1)c$ with $m > 0$. The observer *O'* emits light in the direction *x, x'* and both *O* and *O'* observe and measure the propagation velocity of the same. For *O*, in the speed 0_coordinate, light always propagates with velocity *c*, but what about the observer *O'*?

As in the previous case, (1) and (2) are fulfilled for *O*. While, from the point of view of *O'*, (3) is fulfilled. We will make use of the LTm equations, according to the ER [7], that is,

$$\left.\begin{aligned} x' &= [(m+1)x - vt]\gamma_m \\ y' &= y \\ z' &= z \\ t' &= \left[t - \frac{vx}{(m+1)c^2}\right]\gamma_m \end{aligned}\right\} \text{, with } \gamma_m = \left[(m+1)^2 - \frac{v^2}{c^2}\right]^{-1/2} \tag{8}$$

Where γ_m is the Lorentz factor in the speed m_coordinate.

If we use the descriptive equation of time, according to LTm in the ER (8), multiplying by the parameter *(m+1)c*, we obtain,

$$(m+1)ct' = \left((m+1)ct - \frac{vx}{c}\right)\gamma_m \quad (9)$$

Introducing (1) and (2) in (9),

$$(m+1)ct' = ((m+1)x - vt)\gamma_m \quad (10)$$

So, using the descriptive equation of position, according to LTm in the ER (8), in (10) we obtain,

$$(m+1)ct' = x' \quad (11)$$

And, definitely, comparing (3) with (11), we get,

$$c' = (m+1)c \quad (12)$$

Which means that even if *O* is an observer moving with lower speed to *c* and always measure the light with speed *c*, does not mean that any other observer *O'* with the possibility of moving with speeds higher than *c*, also measure the light propagation with the same speed. For *O'* the light propagates according to the speed coordinate from where the observer is moving. That is, if *O'* moves in the speed m_coordinate, the light propagates with *(m+1)c*.

The LT perfectly fits the SR and its principles: ERP and constancy of *c*. But, this does not mean that the LT justifies the constancy hypothesis of *c* for every inertial observer. In fact, it is observed with the previous demonstrations that there is the same parallelism between the LTm and the ER, which does not mean that these transformations fully justify the quantization hypothesis of *c*. What can be assured is that the quantization of the speed of light, as described in (12), justifies the possibility of bodies (observers like *O'*) moving with speeds higher than *c*, without being observed properly by observers like *O*, who move with speed less than *c*.

The problem that results from applying the LT in the SR is that, by imposing the constancy hypothesis of *c* and finding formal justification of it with the transformations themselves, according to (7), the SR is closed to other possibilities that, applying LTm in the ER, the latter does offer. Specifically, according to (12) is pointed to the relationship between the quantization of the speed of light (variability) and objects moving with velocity greater than *c*, but without being captured with such velocities by observers of the speed 0_coordinate.

III. Wave Equation Study

Assuming an observer *O'(x',y',z',t')* inside a vehicle in a generic speed m_coordinate, moving with relative speed *v*, such that, $mc \leq v < (m+1)c$ with *m=0,1,2,3,..*, respect to another observer *O(x,y,z,t)* in the positive direction of the *x'* and *x* axis. Observer *O* is in the speed 0_coordinate and the plans $x'y'$ and *xy* always match. At the origin *t'=t=0* (See Fig. 1).

In the beginning *t=0*, *O* emits omnidirectional light with frequency f_0 and wavelength λ_0 producing a spherical wave front that is transmitted with velocity *c*, origin *O* and radius *r=ct*.

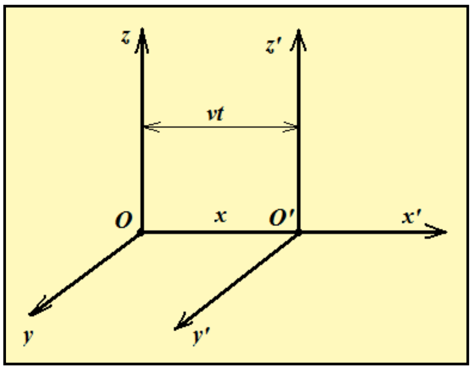

Fig. 1: Context of the experiment: $mc \leq v < (m+1)c$ with *m=0,1,2,3,..*,

The wave emitted in *t=0* in the environment with refractive index *n*, from *O* in the direction *x, x'* is described by,

$$f(x,t) = Asen(\omega_0 t + nK_0 x) \quad (13)$$

With,

$$\omega_0 = 2\pi f_0 \quad (14)$$

$$K_0 = \frac{\omega_0}{c} \quad (15)$$

$$n = \frac{c}{s} \text{ and } s < c \quad (16)$$

Where *s* is the propagation speed in the environment considered.

If we define the partial derivatives $\frac{\partial f(x,t)}{\partial x}, \frac{\partial^2 f(x,t)}{\partial x^2}$ and $\frac{\partial f(x,t)}{\partial t}, \frac{\partial^2 f(x,t)}{\partial t^2}$, it is obtained the typical wave equation in the direction x, x',

$$\frac{\partial^2 f(x,t)}{\partial x^2} = \frac{1}{\rho_{OO}^2}\frac{\partial^2 f(x,t)}{\partial t^2} \quad (17)$$

With,

$$\rho_{OO} = \frac{\omega_0}{K_0 n} = \frac{c}{n} = \text{s} \quad (18)$$

Where ρ_{OO} is the emitted wave speed by *O* and seen from *O* .

We will use the notation $\rho_{\mathbf{AB}}$, where *A* is the emitter of the light (wave) and *B* the observer.

Now, we will apply relativistic Doppler effect [14]. From *O* the wave equation can be written as,

$$\lambda_0 f_0 = c \quad (19)$$

Where λ_0 is the wavelength observed from *O*.

But, from *O'* in the speed_m coordinate the wave equation has the following form,

$$\lambda'_0 f'_0 = (m+1)c \quad (20)$$

O' observes the light with frequency f'_0 and wavelength λ'_0. As *O'* moves going away from *O* with *v*,

$$\lambda'_0 = [(m+1)c - v]T' \quad (21)$$

Where *T'* is the period of the light seen in *O'*. So, applying dilation time generalization [7], we get,

$$T' = T_0\gamma_m \quad (22)$$

T_0 is the period of the light seen from *O* and γ_m is the Lorentz factor in the speed_m coordinate (8).

$$\gamma_m = ((m+1)^2 - \beta^2)^{-1/2} \quad \text{with} \quad \beta = \frac{v}{c} \quad (23)$$

Introducing (22) and (23) in (21),

$$\lambda'_0 = \frac{[(m+1)c-v]T_0}{((m+1)^2-\beta^2)^{1/2}} = \frac{[(m+1)-\beta]\lambda_0}{((m+1)^2-\beta^2)^{1/2}} \quad (24)$$

Substituting wavelengths λ'_0 and λ_0 in (24) by equivalent frequencies, using (19) and (20),

$$\frac{f'_0}{(m+1)c} = \frac{f_0}{c}\frac{((m+1)^2-\beta^2)^{1/2}}{(m+1)-\beta} \quad (25)$$

Rearranging (25) we obtain the results of the relativistic Doppler effect, being the source *O* and the observer *O'* in different speed coordinates,

$$f'_0 = f_0(m+1)\left(\frac{(m+1)+\beta}{(m+1)-\beta}\right)^{1/2} \quad (26)$$

From *O'(x',y',z',t')*, signal $f(x,t)$ is seen as one wave $f'(x',t')$ defined as follows,

$$f'(x',t') = Asen(\omega'_0 t + nK'_0 x') \quad (27)$$

$$\omega'_0 = 2\pi f'_0 = 2\pi f_0(m+1)\left(\frac{(m+1)+\beta}{(m+1)-\beta}\right)^{\frac{1}{2}} = \omega_0(m+1)\left(\frac{(m+1)+\beta}{(m+1)-\beta}\right)^{\frac{1}{2}}, \text{with } \beta = \frac{v}{c} \quad (28)$$

$$K'_0 = \frac{\omega'_0}{(m+1)c} = K_0\left(\frac{(m+1)+\beta}{(m+1)-\beta}\right)^{1/2} \quad (29)$$

Substituting (8) of the Lorentz transformations for speed_m coordinate in (27), with (28) and (29),

$$f'(x,t) = Asen\left[\left(\omega_0(m+1)\left(t - \frac{vx}{(m+1)c^2}\right) + nK_0((m+1)x - vt)\right)\frac{1}{(m+1)-\beta}\right] \quad (30)$$

If we define the partial derivatives $\frac{\partial f'(x,t)}{\partial x}, \frac{\partial^2 f'(x,t)}{\partial x^2}$ and $\frac{\partial f'(x,t)}{\partial t}, \frac{\partial^2 f'(x,t)}{\partial t^2}$, it is obtained the wave equation in the direction x, x' for the observer O', seeing the light emitted by *O*,

$$\frac{\partial^2 f'(x,t)}{\partial x^2} = \frac{1}{\rho_{OO'}^2}\frac{\partial^2 f'(x,t)}{\partial t^2} \quad (31)$$

With,

$$\rho_{OO'} = \frac{\omega_0(m+1) - nK_0}{-\omega_0(m+1)(v/(m+1)c^2) + (m+1)nK_0} \quad (32)$$

If we rewrite the equation (32), considering that,

$$\frac{\omega'_0}{nK'_0} = \frac{\omega_0(m+1)}{nK_0} = (m+1)s \quad (33)$$

We obtain,

$$\rho_{OO'} = \frac{\frac{\omega_0(m+1)}{nK_0} - v}{(m+1) - \frac{\omega_0(m+1)v}{(m+1)c^2 nK_0}} = \frac{s(m+1)-v}{(m+1)-\frac{v}{s}} = \frac{s(s(m+1)-v)}{s(m+1)-v} = s, \ \forall m \quad (34)$$

Equation (34) applied in a vacuum, where $s=c$, means that from O' the light wave is seen with speed $\rho_{OO'} = \rho_{OO} = c$. In other different environments, $\rho_{OO'} = s$.

If the wave is emitted by O' , the observer O' would see it propagating with speed $\rho_{O'O'}$.

If we define the partial derivatives $\frac{\partial f'(x',t')}{\partial x'}, \frac{\partial^2 f'(x',t')}{\partial x'^2}$ and $\frac{\partial f'(x',t')}{\partial t'}, \frac{\partial^2 f'(x',t')}{\partial t'^2}$, over (27), it is obtained the propagating speed $\rho_{O'O'}$ of the wave in the direction *x*, *x'* for the observer *O'*, seeing the light emitted by *O'*,

$$\rho_{O'O'} = \left(\frac{\frac{\partial^2 f'(x',t')}{\partial t'^2}}{\frac{\partial^2 f'(x',t')}{\partial x'^2}}\right)^{1/2} = \frac{\omega'_0}{nK'_0} = \frac{\omega_0(m+1)}{nK_0} = s(m+1)\ ,\forall m \qquad (35)$$

Finally, let's consider how the situation is described when *O'* emits the light and is observed by *O*.

Equations (8) can be written for *x* and *t*, such as:

$$\left.\begin{aligned} x &= \frac{\frac{x'}{\gamma_m}+vt}{m+1} \\ t &= \frac{t'}{\gamma_m} + \frac{vx}{(m+1)c^2} \end{aligned}\right\} \qquad (36)$$

Which rearranged, give rise to (37),

$$\left.\begin{aligned} x &= \frac{x'}{(m+1)\gamma_m} + \frac{vt'}{(m+1)\gamma_m} + x\frac{v^2}{(m+1)^2c^2} \Rightarrow x\left(1-\frac{v^2}{(m+1)^2c^2}\right) = \frac{x'+vt'}{(m+1)\gamma_m} \Rightarrow x = (m+1)\gamma_m(x'+vt') \\ t &= \frac{t'}{\gamma_m} + \frac{vx'}{\gamma_m(m+1)^2c^2} + t\frac{v^2}{(m+1)^2c^2} \Rightarrow t\left(1-\frac{v^2}{(m+1)^2c^2}\right) = \frac{t'}{\gamma_m} + \frac{vx'}{\gamma_m(m+1)^2c^2} \Rightarrow t = \gamma_m\left((m+1)^2t' + x'\frac{v}{c^2}\right) \end{aligned}\right\}$$

The light emitted by *O'* is seen by *O* in the *x*-direction as a wave $f(x',t')$ described as follows, substituting in (13), equations (28), (29) and (37),

$$f(x',t') = Asen\left[\left(\frac{\omega'_0}{m+1}\left((m+1)^2t' + x'\frac{v}{c^2}\right) + nK'_0(m+1)(x'+vt')\right)\frac{1}{(m+1)+\beta}\right] \qquad (37)$$

Then the light from *O* is seen propagating with speed,

$$\rho_{O'O} = \left(\frac{\frac{\partial^2 f(x',t')}{\partial t'^2}}{\frac{\partial^2 f(x',t')}{\partial x'^2}}\right)^{\frac{1}{2}} = \frac{\frac{\omega'_0}{m+1}(m+1)^2 + nK'_0(m+1)v}{\frac{\omega'_0}{(m+1)c^2}\frac{v}{} + nK'_0(m+1)} =$$

$$= \frac{\frac{\omega'_0}{nK'_0}(m+1) + (m+1)v}{\frac{\omega'_0}{(m+1)nK'_0}\frac{v}{c^2} + (m+1)} = \frac{(m+1)^2s + (m+1)v}{\frac{v}{s} + (m+1)} = \frac{[(m+1)s+v]s}{(m+1)s+v} = s\ ,\forall m \qquad (38)$$

In conclusion:

- Regardless of the speed coordinate where the observer is, (18) with observer *O* and (34) with observer *O'*, the wave emitted from the speed 0_coordinate is always propagated at velocity *s* (in the vacuum, *s=c*).

$\rho_{OO}=\rho_{OO'}=s,\ \forall m$ (39)

- But also, $\rho_{O'O}=s, \forall m$. What corroborates the hypothesis about quantization of light, unobservable from the speed 0_coordinate, where always light propagates with speed *s*. Equation (38) tells us that although the light propagates in the speed m_coordinate with velocity *(m+1)s*, from the speed 0_coordinate the observer *O* sees it at velocity *s* (in a vacuum, $s = c$).
- However, $\rho_{O'O'}=(m+1)s, \forall m$. That is, from the speed m_coordinate light propagating at velocity *(m+1)s*, is seen with this same real velocity (35).

IV. Theory About Harmonic Spectral Analysis Experiments

A spectrum analyzer is calibrated in amplitude by injecting it with an amplitude signal that is known with great accuracy, using a given reference frequency. For this, a signal is generated controlled in voltage (or power) and frequency of the least possible distortion, using the same output impedance as the input to the analyzer. Thus, we make sure that the generated control signal concentrates practically all its power in the fundamental harmonic, since for a practical distortion close to zero the power absorbed by higher order harmonics is negligible, compared to that of the fundamental harmonic, even for small level signals. The amplitude of the signal displayed at the control frequency (that of the fundamental harmonic) is adjusted in the analyzer with the known control amplitude value.

Let's now assume that we generate any signal with power *P* over 50Ω impedance. It is injected into a spectrum analyzer with the same input impedance trying to determine its power, named as *P'*, as well as to what extent it differs from that of the generator, that is, the power difference *(P-P')*.

Considering the signal composed of harmonics, in fact, by the sum of *(j+1)* significant harmonics [15], we have that the input power *P* to the analyzer can be defined as,

$$P = P_0 + P_1 + P_2 + .. + P_j = \sum_{i=0}^{j} P_i \qquad (40)$$

P_0 is the fundamental harmonic power and P_i the power of the generic *i* harmonic, with *i=0,1,.., j*.

The power of the signal with frequency *f* which for each cycle displaces *n* particles associated with an energy *E* [16], can be described as,

$$P = \frac{E}{t} = \frac{nhf}{T} = nhf^2 = nK\ \text{, with } K = hf^2 \text{ and } T = 1/f \qquad (41)$$

Where the signal of frequency *f* has period *T*, associated with *n* particles, being *h* the Planck's constant.

The input power P generated to the spectrum analyzer is distributed in harmonics [17], each associated with a number of specific particles, whose energy is a function of the harmonic frequency. Thus, from the analyzer by tuning the central frequency f, the power signal P is obtained distributed in j significant harmonics of individual powers $P_0, P_1, .., P_j$, which in turn displace $n_0, n_1, .., n_j$ particles, respectively, such that for each P_i input to the analyzer and considering speed 0_coordinate reference, you have,

$$P_i = n_i \hbar f_i f \text{ with } P_0 = n_0 K \text{ , } P_1 = 2n_1 K \text{ , ...,} P_j = (1+j)n_j K \quad (42)$$

Observe that the energy E_i of each power harmonic P_i, such that,

$$P_i = E_i f \quad (43)$$

It takes the following value,

$$E_i = n_i \hbar f_i \text{ with } i = 0,1,..,j \quad (44)$$

That is, the n_i particles associated with each harmonic of frequency f_i can be captured as $(1+i)n_i$ particles at frequency f, since their energy described in (44) can also be set as,

$$E_i = (1+i)n_i \hbar f \text{ with } i = 0,1,..,j \text{ and } f_i = (1+i)f \quad (45)$$

Now, the speed coordinate quantization theory establishes that the wavelength λ of each i harmonic of frequency f_i is the same, when using a propagation velocity of $(i+1)c$ in each of them [7]. Therefore, the generated power P_i supplied to each harmonic containing energy E_i is applied over a period T_i, such that,

$$P_i = \frac{E_i}{T_i} \text{ with } i = 0,1,..,j \quad (46)$$

That is, (46) substitutes (43), with relative reference to each i harmonic, so that,

$$(i+1)c = \frac{\lambda}{T_i} \quad (47)$$

And how,

$$c = \frac{\lambda}{T} \quad (48)$$

If T is the period associated with the signal frequency f, then, combining (47) and (48),

$$T_i = \frac{T}{i+1} \quad (49)$$

So, by entering (49) in (46) and using (45), you get,

$$P_i = \frac{E_i(i+1)}{T} = E_i(i+1)f = n_i(i+1)^2 K \quad (50)$$

Therefore, (50) substitutes (42), now being the relative reference to each i harmonic. Therefore, by applying the speed coordinate quantization theory, signal generation is associated with the following power distribution P,

$$P = \sum_{i=0}^{j} P_i = K\left(n_0 + 4n_1 + 9n_2 + .. + (1+j)^2 n_j\right) = nK \text{ , with } n = \sum_{i=0}^{j}(1+i)^2 n_i \quad (51)$$

On the other hand, in practice it is possible to differentiate between the harmonic distribution of the generated power P (Fig.2) and the power measurement in each of these harmonics P_i' with the spectral analysis (Fig.3), such that, the total spectral measurement P' is obtained as follows,

$$P' = \sum_{i=0}^{j} P'_i \quad (52)$$

Experimentally, it is observed that the input power P generated does not match with the measured power P' after the spectral analysis, so that,

$$P > P' \quad (53)$$

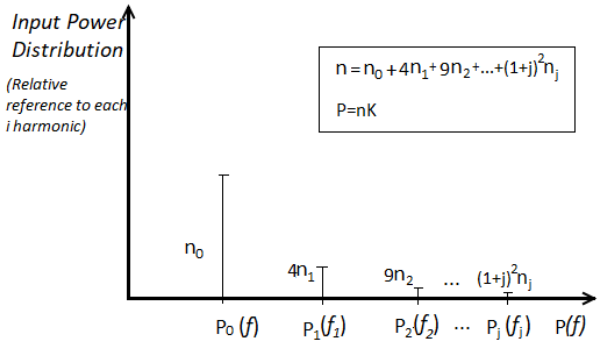

Fig. 2: Power P harmonic distribution generated at the spectrum analyzer input, with reference to each i harmonic.

The result of the image in Fig. 3 is obtained by applying the following considerations,

1. At the input to the analyzer, the power P is distributed according to (51) with relative reference to each i harmonic. That is, P_0 for the 0 harmonic in the speed 0_coordinate, P_1 for the 1 harmonic in the speed 1_coordinate, and so on.

But it turns out that the experimental spectral measurements indicate that *P>P'*, because they are made in the speed 0_coordinate, that is, all of them with reference to the fundamental *0* harmonic.

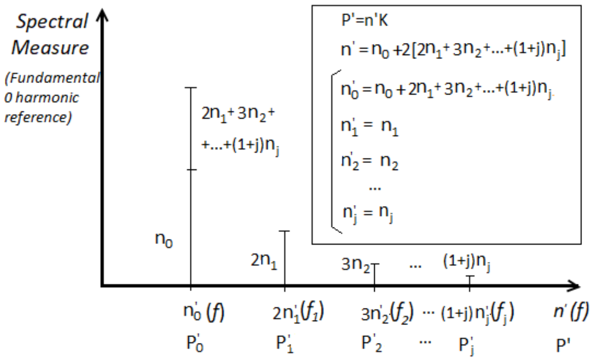

For each *i* harmonic:
- n_i particles generated, according to the power distribution *P* of the input signal.
- n'_i particles measured by spectral analysis for power *P'*.

Fig. 3: Harmonic distribution of the power *P'* measured with the spectral analysis and speed 0_coordinate reference.

2. Using the speed coordinate quantization theory, trying to solve the previous situation, you get:
   a. Each *i* harmonic and its associated particles n_i move to $(i+1)c$ velocity.
   b. When measuring by tuning in the frequency *f* with reference to the speed 0_coordinate in the fundamental harmonic, we observe the contribution of P_0 with n_0 particles, but also the contribution of the rest of the higher order harmonics, as if they were moving at velocity *c*, that is, with $P_1, P_2, .., P_j$. The total power observed in the fundamental harmonic contribution from all the harmonics, not only from the fundamental, is what has been named as P_0' associated to n'_0 particles. Thus, it is obtained as a spectral measure in the fundamental harmonic,

$$P'_0 = n'_0 K \tag{54}$$

Where the number of particles n'_0 associated with the power P'_0 is,

$$n'_0 = \left(n_0 + 2n'_1 + 3n'_2 + .. + (1+j)n'_j\right) \tag{55}$$

   c. Regarding the higher order harmonics measured spectrally from the speed 0_coordinate, taking as reference the fundamental harmonic, they give rise to individual powers $P'_1, .., P'_j$ which in turn displace $n'_1, .., n'_j$ particles, respectively, such that, for each P'_i measured in the analyzer, we have,

$P'_i = n'_i \hbar f_i f$, such that $i=0,1,..,j$, with $P'_0 = n'_0 K$, $P'_1 = 2n'_1 K$, .., $P'_j = (1+j)n'_j K$ (56)

Therefore, the spectral analysis provides the following power distribution *P'*,

$$P' = \sum_{i=0}^{j} P_i' = K\left(n'_0 + 2n'_1 + 3n'_2 + .. + (1+j)n'_j\right) \text{ with } n' = \sum_{i=0}^{j}(1+j)n'_i \tag{57}$$

Introducing (55) in (57), it is achieved,

$$P' = n'K = K\left[n_0 + 2\left(2n'_1 + 3n'_2 + .. + (1+j)n'_j\right)\right] \tag{58}$$

Where *n'* is the total particles number associated with the total power *P'* measured spectrally.

3. On the other hand, what is the relationship between particles n_i distributed in each harmonic by the generated input signal and the number of particles n'_i observed in each harmonic with the spectral analysis?
   a. At the frequency of the fundamental harmonic, n'_0 particles are observed, whose value is given by (55). That is, it is the contribution from the fundamental harmonic with n_0 particles at frequency *f*, but also the rest one from the higher order harmonics observed as $n'_1, n'_2, .., n'_j$, at frequencies $f_1, f_2, .., f_j$, respectively, where the f_i/T parameter at the speed 0_coordinate used in the observation gives rise to $2f^2, 3f^2, .., (1+j)f^2$, respectively.
   b. In the higher order harmonics we can observe $(1+i)n'_i$ particles for each *i* harmonic associated to each frequency $f_i=(i+1)f$, with temporal reference *T* (the measurements are at the speed 0_coordinate). Since the particles distributed in each higher order harmonic by the input signal take values $(1+i)n_i$ or for each frequency f_i with reference to *T(f)*, then the measurement observed with reference to each f_i is also $(1+i)n_i$. Therefore, considering the definition of *n'* obtained with the spectral observation by (57), it is concluded that,

$$n'_i = n_i , \forall i > 0 \tag{59}$$

Relating the powers described in (51) with the measurements according to (57),

$$\frac{P'}{P} = \frac{n'}{n} \tag{60}$$

Thus, using the definition of *n* in (51) and that of *n'* in (57) with (59) and introducing them in (60),

$$\frac{P'}{P}=\frac{n'_0+2n'_1+3n'_2+..+(1+j)n'_j}{n_0+4n_1+9n_2+..+(1+j)^2n_j}=\frac{n_0+2(2n_1+3n_2+..+(1+j)n_j)}{n_0+4n_1+9n_2+..+(1+j)^2n_j}=\frac{n_0+2\sum_{i=0}^{j}(1+i)n_i}{\sum_{i=0}^{j}(1+i)^2n_i} \quad (61)$$

Giving place, with respect to each harmonic, to the following power relationships,

$$\frac{P'_0}{P_0}=\frac{\sum_{i=0}^{j}(1+i)n_i}{n_0} \quad (62)$$

$$\frac{P'_1}{P_1}=\frac{1}{2}\ ,\ \frac{P'_2}{P_2}=\frac{1}{3}\ ,.. \quad (63)$$

$$\frac{P'_j}{P_j}=\frac{1}{(1+j)}\ ,\forall j>0 \quad (64)$$

The observation expressed in (53) can be quantized in the form of a power difference *D*, between the generation *P* distributed into different speed coordinates and the observed *P'* measured from the speed 0_coordinate. Using (51), (58) and (59), you get,

$$D=P-P'=K\left(3n_2+8n_3+..+[(1+j)^2-2(1+j)]n_j\right)=K\sum_{i=2}^{j}[(1+i)^2-2(1+i)]n_i \quad (65)$$

On the other hand, it is also important to express the power difference between the fundamental harmonics, measured with power P'_0 and generated with power P_0. Thus, using (51), (54), (55) and (59), D_0 is obtained,

$$D_0=P'_0-P_0=K\left(2n_1+3n_2+..+(1+j)n_j\right)=K\sum_{i=1}^{j}(1+i)n_i \quad (66)$$

So, according to (65) and (66), in the power differences *D* and D_0, the value of the fundamental harmonic does not intervene, and in *D*, neither that of the first higher order harmonic. This means the following:

- For signals of the same level and frequency, *D* and D_0 will be greater, the greater the distortion; that is, comparing a square signal with a sinusoidal one with both same frequency and level, the square one must produce higher *D* and D_0.
- On the other hand, in the values of *D* and D_0, the parameter *K* also influences, function of f^2, therefore, for the same signal shape and level, the higher frequency, *D* and D_0 will be greater.

  In addition, it is concluded that:
- The definition of *D* according to (65) explains why in practice it is detected that $P>P'$ (53), so that its numerical value is influenced by the signal shape (degree of distortion) and frequency.
- The definition of D_0 according to (66) determines that $P'_0>P_0$, so that, the fundamental harmonic observed has always more power than the fundamental harmonic generated.

V. Experiment1

The aim is to perform a spectral analysis of a sinusoidal signal generated at different frequencies and with an unique level. With the spectral analysis it is possible to measure harmonic powers and their sum is compared with the power of the generated input signal. In addition, the power of the fundamental harmonic measured will be compared with respect to the calculated theoretical one. The number of particles *n'* and *n* are defined, associated with measured powers and theoretical powers, respectively.

An unique generator of very low distortion sinusoidal signals [18] will be used for all measurements. The precision level of the experiment is given by the first ten harmonics measurement of each signal (except in 250MHz, where only six harmonics are used). Thus, the power distribution measured with respect to each signal of frequency *f*, up to 100MHz, will be $P'_0, P'_1, .., P'_9$, in *f, 2f,..,10f*, respectively.

The powers obtained applying (40) and (51), on the one hand and, (57) on the other hand, are,

$$P\approx\sum_{i=0}^{9}P_i=K(n_0+4n_1+9n_2+..+100n_9) \quad (67)$$

$$P'\approx\sum_{i=0}^{9}P_i{}'=K(n'_0+2n'_1+3n'_2+..+10n'_9) \quad (68)$$

Where *P* is the input power and *P'* is the measured power.

That is, using (55) and (59) in (68),

$$P'\approx\hbar f^2(n_0+2n_1+..+10n_9)+\hbar f_1f_1n_1+..+\hbar f_9f_9n_9=K[n_0+2(2n_1+3n_2+..+10n_9)] \quad (69)$$

Where *n'* and *n* are the total particles number associated with the powers of the generated input signal and the measured analyzed signal, respectively, defined as,

$$n'=\sum_{i=0}^{9}(1+j)n'_i=n'_0+2n'_1+..+10n'_9=n_0+4n_1+6n_2+..+20n_9 \quad (70)$$

$$n=\sum_{i=0}^{9}(1+i)^2n_i=n_0+4n_1+9n_2+..+100n_9 \quad (71)$$

Sinusoidal inputs with 50Ω impedance will be always applied to the Rigol DSA815TG spectrum analyzer [19] at different frequencies and amplitude of *317mVrms* (*3dBm*). Selective level measurements will be carried out in "zero scan" mode, where the analyzer functions as a heterodyne receiver with selectable bandwidth, through the center frequency. Power measurements of the first ten harmonics referred to 50Ω impedance are obtained.

We will use a system of eleven equations described by the ten measurements taken plus the equation corresponding to the input power (for 250MHz are only seven equations), that is,

$$\left.\begin{aligned} P'_0 &= (n_0 + 2n_1 + 3n_2 + .. + 10n_9 + 11n_{10})K \\ P'_1 &= 2n_1 K \\ &\ldots\ldots \\ P'_9 &= 10n_9 \\ P &= (n_0 + 4n_1 + 9n_2 + .. + 100n_9 + 121n_{10})K \end{aligned}\right\} \quad (72)$$

The unknowns are ten n_i for $i=0,1,..,9$, which multiplied by the coefficient $K(i+1)^2$ provide the input power value of each P_i for $i=0,1,..,9$.

The number eleven unknown n_{10} is associated with the rest power of the higher order harmonics from the tenth of the input signal. That is, P_{10} is not the tenth harmonic power but the rest power of the higher order harmonics not considered after the tenth, including this one.

We will name P_{10} as the rest input power for frequencies up to 100MHz:

$$P_{rest} = P_{10} = 121n_{10}K \quad (73)$$

With the particles number n_i associated with each harmonic of frequency f_i, we can obtain *P'*. From *P'* and, since *P* has an imposed value (*3dBm*), the power difference between the input *P* (with *n* particles) and the measured power *P'* (with *n'* particles) (65) is determined. Also from P_0 and P'_0, the difference D_0 (66) is achieved.

The results obtained are shown in Table1 and Table2.

Table 1: Data and results of the experiment1 from 50KHz to 1MHz.

f_0/P(dBm,μw)/THD/ K=hf_0^2/(RBW)				50KHz / (3dBm, 2010μw) / 0.27% / 16.565 10^{-25}w / (300Hz)						
P_0' μw/dBm	***P_1'*** nw/dBm	***P_2'*** nw/dBm	***P_3'*** nw/dBm	***P_4'*** nw/dBm	***P_5'*** nw/dBm	***P_6'*** nw/dBm	***P_7'*** nw/dBm	***P_8'*** nw/dBm	***P_9'*** nw/dBm	
1506.61/ 1.78dBm	8.71/ -50.6dBm	2/ -56.99dBm	0.048/ -73.18dBm	0.099/ -70.03dBm	0.026/ -75.84dBm	0.025/ -75.98dBm	0.021/ -76.78dBm	0.026/ -75.82dBm	0.015/ -78.21dBm	
n_0K(μw)/ P_0(μw)	***n_1K(nw)/ P_1(nw)***	***n_2K(nw)/ P_2(nw)***	***n_3K(nw)/ P_3(nw)***	***n_4K(nw)/ P_4(nw)***	***n_5K(nw)/ P_5(nw)***	***n_6K(nw) /P_6(nw)***	***n_7K(nw) /P_7(nw)***	***n_8K(nw) /P_8(nw)***	***n_9K(nw) /P_9(nw)***	***n_{10}K(μw)/ P_{10}(μw)***
1456.26/ 1456.26	4.355/ 17.42	0.667/ 6	0.012/ 0.192	0.0198/ 0.495	0.0043/ 0.1560	0.00357/ 0.1750	0.00263/ 0.1680	0.0029/ 0.2340	0.0015/ 0.15	4.576/ 553.72
P' (μw)				***D=P- P'(μw)***		***D_0=P_0'- P_0(μw)***				
P_0'+10.97nw=1506.611				503.39		50.35				
f_0/P(dBm,μw)/THD/ K=hf_0^2/(RBW)				100KHz / (3dBm, 2010μw) / 0.25% / 6.626 10^{-24}w / (300Hz)						
P_0' μw/dBm	***P_1'*** nw/dBm	***P_2'*** nw/dBm	***P_3'*** nw/dBm	***P_4'*** nw/dBm	***P_5'*** nw/dBm	***P_6'*** nw/dBm	***P_7'*** nw/dBm	***P_8'*** nw/dBm	***P_9'*** nw/dBm	
1570.36/ 1.96dBm	7.853/ -51.05dBm	1.663/ -57.79dBm	0.020/ -77.06dBm	0.029/ -75.37dBm	0.018/ -77.48dBm	0.025/ -76.05dBm	0.014/ -78.42dBm	0.019/ -77.13dBm	0.015/ -78.33dBm	
n_0K(μw)/ P_0(μw)	***n_1K(nw)/ P_1(nw)***	***n_2K(nw)/ P_2(nw)***	***n_3K(nw)/ P_3(nw)***	***n_4K(nw)/ P_4(nw)***	***n_5K(nw)/ P_5(nw)***	***n_6K(nw) /P_6(nw)***	***n_7K(nw) /P_7(nw)***	***n_8K(nw) /P_8(nw)***	***n_9K(nw) /P_9(nw)***	***n_{10}K(μw)/ P_{10}(μw)***
1526.39/ 1526.39	3.927/ 15.706	0.554/ 4.989	0.005/ 0.08	0.0058/ 0.145	0.003/ 0.108	0.0036/ 0.1750	0.00175/ 0.112	0.0021/ 0.171	0.0015/ 0.15	3.997/ 483.59
P' (μw)				***D=P- P'(μw)***		***D_0=P_0'- P_0(μw)***				
P_0'+9.656nw=1570.37				439.63		43.97				
f_0/P(dBm,μw)/THD/ K=hf_0^2/(RBW)				1MHz / (3dBm, 2010μw) / 0.21% / 6.626 10^{-22}w / (3KHz)						
P_0' μw/dBm	***P_1'*** nw/dBm	***P_2'*** nw/dBm	***P_3'*** nw/dBm	***P_4'*** nw/dBm	***P_5'*** nw/dBm	***P_6'*** nw/dBm	***P_7'*** nw/dBm	***P_8'*** nw/dBm	***P_9'*** nw/dBm	
1462.18/ 1.65dBm	5.24/ -52.81dBm	0.5370/ -62.70dBm	0.0755/ -71.22dBm	0.1368/ -68.64dBm	0.0603/ -72.20dBm	0.1439/ -68.42dBm	0.0526/ -72.79dBm	0.0918/ -70.37dBm	0.0468/ -73.30dBm	
n_0K(μw)/ P_0(μw)	***n_1K(nw)/ P_1(nw)***	***n_2K(nw)/ P_2(nw)***	***n_3K(nw)/ P_3(nw)***	***n_4K(nw)/ P_4(nw)***	***n_5K(nw)/ P_5(nw)***	***n_6K(nw) /P_6(nw)***	***n_7K(nw) /P_7(nw)***	***n_8K(nw) /P_8(nw)***	***n_9K(nw) /P_9(nw)***	***n_{10}K(μw)/ P_{10}(μw)***
1407.40/ 1407.40	2.62/ 10.48	0.179/ 1.611	0.0189/ 0.302	0.0274/ 0.684	0.0101/ 0.3618	0.0206/ 1.007	0.0066/ 0.4208	0.0102/ 0.8262	0.00468/ 0.468	4.98/ 602.59
P' (μw)				***D=P- P'(μw)***		***D_0=P_0'- P_0(μw)***				
P_0'+6.386nw=1462.19				547.81		54.78				

Table3 shows the results processed that give rise to the following conclusions:

- For the same signal level, the power difference *D* of the input power with respect to the measurement increases with the frequency increase, in general. Increasing the frequency with a sufficient decrease of the *THD* can cause the power difference *D* decreasing.
- The conclusions obtained for the power difference D_0 between the measured fundamental harmonic and the input fundamental harmonic are the same as for *D*. In general, the increase in frequency for the same signal level and progressive increments of *THD* produces an increase in D_0.
- For the same signal level, the *D/P* and D_0/P_0' ratios in percentage increase with the increase in frequency, in general, as long as *THD* increments are maintained.

Table 2: Data and results of the experiment1 from 10MHz to 250MHz.

f_0/P(dBm,μw)/THD/ $K=hf_0^2$/(RBW)				10MHz / (3dBm, 2010μw) / 0.19% / 6.626 10^{-20}w / (30KHz)						
P_0' μw/dBm	***P_1'*** nw/dBm	***P_2'*** nw/dBm	***P_3'*** nw/dBm	***P_4'*** nw/dBm	***P_5'*** nw/dBm	***P_6'*** nw/dBm	***P_7'*** nw/dBm	***P_8'*** nw/dBm	***P_9'*** nw/dBm	
1472.31/ 1.68dBm	0.3606/ -64.43dBm	3.013/ -55.21dBm	0.3412/ -64.67dBm	0.2818/ -65.50dBm	0.2897/ -65.38dBm	0.3006/ -65.22dBm	0.3133/ -65.04dBm	0.3296/ -64.82dBm	0.3243/ -64.89dBm	
n_0K(μw)/ P_0(μw)	***n_1K(nw)/ P_1(nw)***	***n_2K(nw)/ P_2(nw)***	***n_3K(nw)/ P_3(nw)***	***n_4K(nw)/ P_4(nw)***	***n_5K(nw)/ P_5(nw)***	***n_6K(nw) /P_6(nw)***	***n_7K(nw) /P_7(nw)***	***n_8K(nw) /P_8(nw)***	***n_9K(nw) /P_9(nw)***	***$n_{10}K$(μw)/ P_{10}(μw)***
1418.54/ 1418.54	0.1803/ 0.7212	1.0043/ 9.040	0.0853/ 1.3648	0.05636/ 1.409	0.04828/ 1.7382	0.0429/ 2.1042	0.03916/ 2.5064	0.0366/ 2.9664	0.0324/ 3.243	4.888/ 591.44
P' (μw)			***D=P- P'(μw)***			***D_0=P_0'- P_0(μw)***				
P_0'+5.54nw=1472.32			537.50			53.77				
f_0/P(dBm,μw)/THD/ $K=hf_0^2$/(RBW)				50MHz / (3dBm, 2010μw) / 0.88% / 16.565 10^{-19}w / (100KHz)						
P_0' μw/dBm	***P_1'*** nw/dBm	***P_2'*** nw/dBm	***P_3'*** nw/dBm	***P_4'*** nw/dBm	***P_5'*** nw/dBm	***P_6'*** nw/dBm	***P_7'*** nw/dBm	***P_8'*** nw/dBm	***P_9'*** nw/dBm	
1406.05/ 1.48dBm	8.8105/ -50.55dBm	84.918/ -40.71dBm	2.3659/ -56.26dBm	1.9231/ -57.16dBm	1.8281/ -57.38dBm	2.0324/ -56.92dBm	2.2029/ -56.57dBm	2.2909/ -56.40dBm	2.2962/ -56.39dBm	
n_0K(μw)/ P_0(μw)	***n_1K(nw)/ P_1(nw)***	***n_2K(nw)/ P_2(nw)***	***n_3K(nw)/ P_3(nw)***	***n_4K(nw)/ P_4(nw)***	***n_5K(nw)/ P_5(nw)***	***n_6K(nw) /P_6(nw)***	***n_7K(nw) /P_7(nw)***	***n_8K(nw) /P_8(nw)***	***n_9K(nw) /P_9(nw)***	***$n_{10}K$(μw)/ P_{10}(μw)***
1345.57/ 1345.57	4.40525/ 17.621	28.306/ 254.754	0.5915/ 9.4636	0.38462/ 9.6155	0.30468/ 10.9686	0.29034/ 14.227	0.2754/ 17.623	0.2545/ 20.618	0.2296/ 22.962	5.488/ 664.05
P' (μw)			***D=P- P'(μw)***			***D_0=P_0'- P_0(μw)***				
P_0'+108.67nw=1406.16			603.85			60.48				
f_0/P(dBm,μw)/THD/ $K=hf_0^2$/(RBW)				100MHz / (3dBm, 2010μw) / 0.49% / 6.626 10^{-18}w / (300KHz)						
P_0' μw/dBm	***P_1'*** nw/dBm	***P_2'*** nw/dBm	***P_3'*** nw/dBm	***P_4'*** nw/dBm	***P_5'*** nw/dBm	***P_6'*** nw/dBm	***P_7'*** nw/dBm	***P_8'*** nw/dBm	***P_9'*** nw/dBm	
1402.81/ 1.47dBm	11.2719/ -49.48dBm	6.9024/ -51.61dBm	1.86209/ -57.30dBm	1.803/ -57.44dBm	1.766/ -57.53dBm	1.875/ -57.27dBm	2.1928/ -56.59dBm	2.65461/ -55.76dBm	2.729/ -55.64dBm	
n_0K(μw)/ P_0(μw)	***n_1K(nw)/ P_1(nw)***	***n_2K(nw)/ P_2(nw)***	***n_3K(nw)/ P_3(nw)***	***n_4K(nw)/ P_4(nw)***	***n_5K(nw)/ P_5(nw)***	***n_6K(nw) /P_6(nw)***	***n_7K(nw) /P_7(nw)***	***n_8K(nw) /P_8(nw)***	***n_9K(nw) /P_9(nw)***	***$n_{10}K$(μw)/ P_{10}(μw)***
1342.07/ 1342.07	5.636/ 22.544	2.3008/ 20.7072	0.46552/ 7.44836	0.3606/ 9.015	0.2943/ 10.596	0.2679/ 13.125	0.2741/ 17.5424	0.295/ 23.8915	0.2729/ 27.29	5.519/ 667.78
P' (μw)			***D=P- P'(μw)***			***D_0=P_0'- P_0(μw)***				
P_0'+33.05nw=1402.84			607.1			60.74				
f_0/P(dBm,μw)/THD/ $K=hf_0^2$/(RBW)				250MHz / (3dBm, 2010μw) / 0.76% / 414.125 10^{-19}w / (300KHz)						
P_0' μw/dBm	***P_1'*** nw/dBm	***P_2'*** nw/dBm	***P_3'*** nw/dBm	***P_4'*** nw/dBm	***P_5'*** nw/dBm	Only six harmonics are used for 250MHz, due to analyzer limitations				
1358.31/ 1.33dBm	41.8794/ -43.78dBm	22.4906/ -46.48dBm	4.3551/ -53.61dBm	4.42588/ -53.54dBm	6.223/ -52.06dBm	1.5GHz analyzer bandwidth				
n_0K(μw)/ P_0(μw)	***n_1K(nw)/ P_1(nw)***	***n_2K(nw)/ P_2(nw)***	***n_3K(nw)/ P_3(nw)***	***n_4K(nw)/ P_4(nw)***	***n_5K(nw)/ P_5(nw)***	***n_6K(μw)/ P_6(μw)***				
1249.64/ 1249.64	20.9397/ 83.7588	7.4969/ 67.4718	1.08878/ 17.4204	0.8852/ 22.1294	1.03717/ 37.338	15.51/ 760.13	$P_{rest} = P_6 = 49n_6K$			
P' (μw)			***D=P- P'(μw)***			***D_0=P_0'- P_0(μw)***				
P_0'+79.38nw=1358.39			651.5			108.67				

- The values of *D* obtained are appreciable and measurable with a spectrum analyzer, even when the higher order harmonics power is negligible compared to that from the fundamental harmonic, despite the low distortion of the sinusoidal input signals. Even the power difference D_0, corresponding to the fundamental harmonics, is already appreciable.
- In a generic way, with the same signal generator for the same level and type of signal, the distortion increases with the frequency and, thus, the powers in the fundamental harmonic P_0 and P_0' decrease, since the associated particles number n_0 y n_0' also decrease.
- The n_i and P_i values for $i=0,1,..,j$, (in this experiment $j=9$ for all frequencies used, except for 250MHz where $j=5$) are obtained by means of a system with $(j+2)$ equations that offers more precise results, the more amount of harmonics it contains (the greater is *j*). Observe that in the *i* harmonic there are n_i particles associated with the input power P_i, such that,

$$P_i = Kn_i(1+i)^2 \quad \text{with} \quad i=0,1,..,j \tag{74}$$

While the power measured in each *i* harmonic is given by P_i',

$$P_i' = Kn_i(1+i) \quad \text{with} \quad i=0,1,..,j \tag{75}$$

The results indicate that the greater the *i* harmonic considered, the smaller the particles number n_i; however, input power P_i injected increases with respect to its P_i' measured, which decreases. There comes a time when P_i' measured reaches the noise level of the spectrum analyzer and, from here, the measurements are not valid. That is, the analyzer noise level limits the value of *j* used. For the value of *j* used in the measurements, we will obtain a P_j representing the power accumulation distributed to the harmonics above j^{th}, including this one. It is what we have named in (73) as rest input power P_{rest}, which is expressed generically for the j^{th} harmonic as,

$$P_{rest} = P_j = Kn_j(1+j)^2 \qquad (76)$$

The signal generator used Hameg HM8134 uses as internal reference 10MHz and, therefore, it is in this frequency where better results are obtained in terms of *THD*, which is noted in the value of *D/P%*.

Table 3: Processing and results summary of the experiment1.

Results Summary (3dBm) Experiment1				
f_0/THD	***D*(μw)**	***D_0*(μw)**	***D/P %***	***D_0/P_0' %***
50KHz/0.27%	503.39	50.35	25.04	3.34
100KHz/0.25%	439.63	43.97	21.87	2.80
1MHz/0.21%	547.81	54.78	27.25	3.75
10MHz/0.19%	537.5	53.77	26.74	3.65
50MHz/0.88%	603.85	60.48	30.04	4.30
100MHz/0.49%	607.10	60.74	30.20	4.33
250MHz/0.76%	651.50	108.67	32.41	8.00

VI. Experiment2

A comparative spectral analysis will now be carried out using signals generated at different frequencies and an unique effective value with sinusoidal and square shapes. The spectral measurements for each frequency provide different power distributions, taking into account the different distortion when comparing sine and square signals.

Table 4: Data and results of the experiment2 from 50KHz to 10MHz for sinusoidal signals.

f_0/P(dBm,μw)/THD/ K=hf_0^2/(RBW)				50KHz / (3dBm, 2010μw) / 0.24% / 16.565 10^{-25}w / (300Hz)						
P_0' μw/dBm	***P_1'*** nw/dBm	***P_2'*** nw/dBm	***P_3'*** nw/dBm	***P_4'*** nw/dBm	***P_5'*** nw/dBm	***P_6'*** nw/dBm	***P_7'*** nw/dBm	***P_8'*** nw/dBm	***P_9'*** nw/dBm	
1472.31/ 1.68dBm	6.761/ -51.70dBm	1.652/ -57.82dBm	0.043/ -73.69dBm	0.046/ -73.35dBm	0.022/ -76.68dBm	0.018/ -77.38dBm	0.016/ -77.88dBm	0.014/ -78.42dBm	0.012/ -79.12dBm	
n_0K(μw) /P_0(μw)	***n_1K(nw)/ P_1(nw)***	***n_2K(nw)/ P_2(nw)***	***n_3K(nw)/ P_3(nw)***	***n_4K(nw)/ P_4(nw)***	***n_5K(nw)/ P_5(nw)***	***n_6K(nw)/ P_6(nw)***	***n_7K(nw)/ P_7(nw)***	***n_8K(nw) /P_8(nw)***	***n_9K(nw)/ P_9(nw)***	***$n_{10}K$(μw)/ P_{10}(μw)***
1418.53/ 1418.53	3.3805/ 13.522	0.5507/ 4.956	0.01075/ 0.172	0.0092/ 0.23	0.0037/ 0.1320	0.00257/ 0.1260	0.002/ 0.128	0.0016/ 0.126	0.0012/ 0.12	4.89/ 591.45
P' (μw)				***D=P- P'(μw)***		***D_0=P_0'- P_0(μw)***				
P_0'+8.584nw=1472.319				537.68		53.785				
f_0/P(dBm,μw)/THD/ K=hf_0^2/(RBW)				100KHz / (3dBm, 2010μw) / 0.24% / 6.626 10^{-24}w / (300Hz)						
P_0' μw/dBm	***P_1'*** nw/dBm	***P_2'*** nw/dBm	***P_3'*** nw/dBm	***P_4'*** nw/dBm	***P_5'*** nw/dBm	***P_6'*** nw/dBm	***P_7'*** nw/dBm	***P_8'*** nw/dBm	***P_9'*** nw/dBm	
1496.24/ 1.75dBm	6.966/ -51.57dBm	1.626/ -57.89dBm	0.023/ -76.41dBm	0.037/ -74.37dBm	0.016/ -77.98dBm	0.018/ -77.57dBm	0.014/ -78.51dBm	0.019/ -77.13dBm	0.015/ -78.38dBm	
n_0K(μw) /P_0(μw)	***n_1K(nw)/ P_1(nw)***	***n_2K(nw)/ P_2(nw)***	***n_3K(nw)/ P_3(nw)***	***n_4K(nw)/ P_4(nw)***	***n_5K(nw)/ P_5(nw)***	***n_6K(nw)/ P_6(nw)***	***n_7K(nw)/ P_7(nw)***	***n_8K(nw)/ P_8(nw)***	***n_9K(nw)/ P_9(nw)***	***$n_{10}K$(μw)/ P_{10}(μw)***
1444.86/ 1444.86	3.483/ 13.932	0.542/ 4.878	0.00575/ 0.092	0.0074/ 0.185	0.0027/ 0.0960	0.0026/ 0.1260	0.00175/ 0.112	0.00211/ 0.1710	0.0015/ 0.15	4.67/ 565.12
P' (μw)				***D=P- P'(μw)***		***D_0=P_0'- P_0(μw)***				
P_0'+8.734nw=1496.249				513.75		51.38				
f_0/P(dBm,μw)/THD/ K=hf_0^2/(RBW)				1MHz / (3dBm, 2010μw) / 0.16% / 6.626 10^{-22}w / (3KHz)						
P_0' μw/dBm	***P_1'*** nw/dBm	***P_2'*** nw/dBm	***P_3'*** nw/dBm	***P_4'*** nw/dBm	***P_5'*** nw/dBm	***P_6'*** nw/dBm	***P_7'*** nw/dBm	***P_8'*** nw/dBm	***P_9'*** nw/dBm	
1475.71/ 1.69dBm	2.7/ -55.64dBm	0.826/ -60.83dBm	0.0853/ -70.69dBm	0.0702/ -71.54dBm	0.0577/ -72.39dBm	0.0522/ -72.82dBm	0.0731/ -71.36dBm	0.0475/ -73.23dBm	0.0589/ -72.30dBm	
n_0K(μw) /P_0(μw)	***n_1K(nw)/ P_1(nw)***	***n_2K(nw)/ P_2(nw)***	***n_3K(nw)/ P_3(nw)***	***n_4K(nw)/ P_4(nw)***	***n_5K(nw)/ P_5(nw)***	***n_6K(nw)/ P_6(nw)***	***n_7K(nw)/ P_7(nw)***	***n_8K(nw)/ P_8(nw)***	***n_9K(nw)/ P_9(nw)***	***$n_{10}K$(μw)/ P_{10}(μw)***
1422.28/ 1422.28	13.5/ 54	0.275/ 2.48	0.0213/ 0.341	0.014/ 0.351	0.0096/ 0.346	0.0075/ 0.365	0.0091/ 0.585	0.0053/ 0.428	0.0059/ 0.589	4.857/ 587.68
P' (μw)				***D=P- P'(μw)***		***D_0=P_0'- P_0(μw)***				
P_0'+3.98nw=1475.714				534.23		53.43				
f_0/P(dBm,μw)/THD/ K=hf_0^2/(RBW)				10MHz / (3dBm, 2010μw) / 0.21% / 6.626 10^{-20}w / (30KHz)						
P_0' μw/dBm	***P_1'*** nw/dBm	***P_2'*** nw/dBm	***P_3'*** nw/dBm	***P_4'*** nw/dBm	***P_5'*** nw/dBm	***P_6'*** nw/dBm	***P_7'*** nw/dBm	***P_8'*** nw/dBm	***P_9'*** nw/dBm	
1428.89/ 1.55dBm	2.6/ -55.95dBm	1.047/ -59.80dBm	0.9268/ -60.33dBm	0.3229/ -64.91dBm	0.2958/ -65.29dBm	0.3170/ -64.99dBm	0.3258/ -64.87dBm	0.3404/ -64.68dBm	0.3311/ -64.80dBm	
n_0K(μw) /P_0(μw)	***n_1K(nw)/ P_1(nw)***	***n_2K(nw)/ P_2(nw)***	***n_3K(nw)/ P_3(nw)***	***n_4K(nw)/ P_4(nw)***	***n_5K(nw)/ P_5(nw)***	***n_6K(nw)/ P_6(nw)***	***n_7K(nw)/ P_7(nw)***	***n_8K(nw)/ P_8(nw)***	***n_9K(nw)/ P_9(nw)***	***$n_{10}K$(μw)/ P_{10}(μw)***
1370.78/ 1370.78	1.3/ 5.2	0.349/ 3.141	0.2317/ 3.707	0.0646/ 1.6145	0.0493/ 1.7748	0.0453/ 2.219	0.0407/ 2.6064	0.0378/ 3.0636	0.03311/ 3.311	5.2826/ 639.227
P' (μw)			***D=P- P'(μw)***			***D_0=P_0'- P_0(μw)***				
P_0'+6.52nw=1428.897			581.1			58.11				

At the spectrum analyzer input, we are injecting a sine-wave or square signal of frequency between 50KHz and 10MHz, generated with the AD Instruments AD8610 equipment [21], using 50Ω impedance, with level +3dBm (1.796Vpp sinusoidal or 1.268Vpp square, equivalent to 2010μw over 50Ω). In the Rigol DSA815TG spectrum analyzer [19] selective level measurements are made in "zero scan" mode of the first ten harmonics, with RBW between 300Hz and 30KHz. Applying the eleven equations system described in (72) and using the ten measurements taken plus the input power, we obtain the unknowns n_i $(i=0,1,..,9)$, particles number associated with each i harmonic of frequency f_i. The unknown n_{10} is associated with the higher order harmonics rest power from the tenth harmonic in the input signal. Adding the first ten power spectral measurements $P_i'(i=0,1,..,9)$ and P_{rest} , the total power value P' is determined. The sum of the measured powers P' is compared to the power of the original input signal P.

Thus, the power of the fundamental harmonic measured will be compared with respect to the calculated theoretical one. The particles number n' (70) and n (71) associated with measured powers P' and input power P, respectively, are defined.

Table 5: Data and results of the experiment2 from 50KHz to 10MHz for squared signals.

f_0/P(dBm,μw)/THD/ K=hf_0^2/(RBW)	50KHz / (3dBm, 2010μw) / 43.93% / 16.565 10^{-25}w / (300Hz)									
P_0' μw/dBm	***P_1'*** μw/dBm	***P_2'*** μw/dBm	***P_3'*** μw/dBm	***P_4'*** μw/dBm	***P_5'*** μw/dBm	***P_6'*** μw/dBm	***P_7'*** μw/dBm	***P_8'*** μw/dBm	***P_9'*** μw/dBm	
1180.32/ 0.72dBm	0.5559/ -32.55dBm	136.46/ -8.65dBm	0.5572/ -32.54dBm	49.09/ -13.09dBm	0.5508/ -32.59dBm	24.66/ -16.08dBm	0.5445/ -32.64dBm	14.59/ -18.36dBm	0.5383/ -32.69dBm	
n_0K(μw)/ P_0(μw)	***n_1K(μw)/ P_1(μw)***	***n_2K(μw)/ P_2(μw)***	***n_3K(μw)/ P_3(μw)***	***n_4K(μw)/ P_4(μw)***	***n_5K(μw)/ P_5(μw)***	***n_6K(μw)/ P_6(μw)***	***n_7K(μw)/ P_7(μw)***	***n_8K(μw)/ P_8(μw)***	***n_9K(μw)/ P_9(μw)***	***$n_{10}K$(μw)/ P_{10}(μw)***
944.57/ 944.57	0.278/ 1.112	45.487/ 409.380	0.139/ 2.229	9.818/ 245.45	0.0918/ 3.305	3.523/ 172.62	0.068/ 4.356	1.621/ 131.31	0.054/ 5.383	0.746/ 90.291
P' (μw)				***D=P- P'(μw)***		***D_0=P_0'- P_0(μw)***				
P_0'+227.55=1407.87				602.13		235.75				
f_0/P(dBm,μw)/THD/ K=hf_0^2/(RBW)	100KHz / (3dBm, 2010μw) / 43.26% / 6.626 10^{-24}w / (300Hz)									
P_0' μw/dBm	***P_1'*** μw/dBm	***P_2'*** μw/dBm	***P_3'*** μw/dBm	***P_4'*** μw/dBm	***P_5'*** μw/dBm	***P_6'*** μw/dBm	***P_7'*** μw/dBm	***P_8'*** μw/dBm	***P_9'*** μw/dBm	
1199.50/ 0.79dBm	0.5458/ -32.63dBm	134.59/ -8.71dBm	0.5534/ -32.57dBm	48.98/ -13.10dBm	0.54.70/ -32.62dBm	24.32/ -16.14dBm	0.5358/ -32.71dBm	22.60/ -16.46dBm	0.5483/ -32.61dBm	
n_0K(μw)/ P_0(μw)	***n_1K(μw)/ P_1(μw)***	***n_2K(μw)/ P_2(μw)***	***n_3K(μw)/ P_3(μw)***	***n_4K(μw)/ P_4(μw)***	***n_5K(μw)/ P_5(μw)***	***n_6K(μw)/ P_6(μw)***	***n_7K(μw)/ P_7(μw)***	***n_8K(μw)/ P_8(μw)***	***n_9K(μw)/ P_9(μw)***	***$n_{10}K$(μw)/ P_{10}(μw)***
965.77/ 965.77	0.2729/ 1.0916	44.863/ 403.770	0.1384/ 2.2136	9.796/ 244.9	0.0912/ 3.2820	3.4743/ 170.240	0.0670/ 4.2864	2.5111/ 203.40	0.05483/ 5.483	0.04594/ 5.559
P' (μw)				***D=P- P'(μw)***		***D_0=P_0'- P_0(μw)***				
P_0'+233.22=1432.72				577.28		233.73				
f_0/P(dBm,μw)/THD/ K=hf_0^2/(RBW)	1MHz / (3dBm, 2010μw) / 42.71% / 6.626 10^{-22}w / (3KHz)									
P_0' μw/dBm	***P_1'*** μw/dBm	***P_2'*** μw/dBm	***P_3'*** μw/dBm	***P_4'*** μw/dBm	***P_5'*** μw/dBm	***P_6'*** μw/dBm	***P_7'*** μw/dBm	***P_8'*** μw/dBm	***P_9'*** μw/dBm	
1199.50/ 0.79dBm	0.53/ -32.76dBm	131.83/ -8.80dBm	0.58/ -32.37dBm	48.31/ -13.16dBm	0.56/ -32.50dBm	23.02/ -16.38dBm	0.53/ -32.73dBm	13.15/ -18.81dBm	0.49/ -33.07dBm	
n_0K(μw)/ P_0(μw)	***n_1K(μw)/ P_1(μw)***	***n_2K(μw)/ P_2(μw)***	***n_3K(μw)/ P_3(μw)***	***n_4K(μw)/ P_4(μw)***	***n_5K(μw)/ P_5(μw)***	***n_6K(μw)/ P_6(μw)***	***n_7K(μw)/ P_7(μw)***	***n_8K(μw)/ P_8(μw)***	***n_9K(μw)/ P_9(μw)***	***$n_{10}K$(μw)/ P_{10}(μw)***
920.79/ 920.79	0.265/ 1.06	43.94/ 395.49	0.145/ 2.32	9.662/ 241.55	0.093/ 3.360	3.29/ 161.13	0.066/ 4.24	1.46/ 118.35	0.049/ 4.9	0.88/ 106.80
P' (μw)				***D=P- P'(μw)***		***D_0=P_0'- P_0(μw)***				
P_0'+99=1298.5				591.5		228.71				
f_0/P(dBm,μw)/THD/ K=hf_0^2/(RBW)	10MHz / (3dBm, 2010μw) / 21.73% / 6.626 10^{-20}w / (30KHz)									
P_0' μw/dBm	***P_1'*** μw/dBm	***P_2'*** μw/dBm	***P_3'*** μw/dBm	***P_4'*** μw/dBm	***P_5'*** μw/dBm	***P_6'*** μw/dBm	***P_7'*** μw/dBm	***P_8'*** μw/dBm	***P_9'*** μw/dBm	
1145.51/ 0.59dBm	0.31/ -35.10dBm	51.17/ -12.91dBm	0.07/ -41.39dBm	0.90/ -30.47dBm	0.009/ -50.34dBm	0.97/ -30.13dBm	0.024/ -46.19dBm	0.65/ -31.89dBm	0.017/ -47.62dBm	
n_0K(μw)/ P_0(μw)	***n_1K(μw)/ P_1(μw)***	***n_2K(μw)/ P_2(μw)***	***n_3K(μw)/ P_3(μw)***	***n_4K(μw)/ P_4(μw)***	***n_5K(μw)/ P_5(μw)***	***n_6K(μw)/ P_6(μw)***	***n_7K(μw)/ P_7(μw)***	***n_8K(μw)/ P_8(μw)***	***n_9K(μw)/ P_9(μw)***	***$n_{10}K$(μw)/ P_{10}(μw)***
1016.73/ 1016.73	0.155/ 0.62	17.057/ 153.51	0.0175/ 0.28	0.18/ 4.5	0.0015/ 0.054	0.139/ 6.79	0.003/ 0.192	0.072/ 5.85	0.0017/ 0.17	6.79/ 821.31
P' (μw)			***D=P- P'(μw)***			***D_0=P_0'- P_0(μw)***				
P_0'+54.12=1199.63			810.37			128.78				

The results obtained are shown in Table4 and Table5 for sine and square signals, respectively. Table6 shows a summary of results, which give rise to the following conclusions:

- The results associated with Table4 for sine signals are similar to those of experiment1 and lead to the same conclusions: in general, the increase in frequency produces an increase in parameters D and D_0, in addition to increasing the D/P and D_0/P_0' ratios.

- For the same level and same frequency, the shape of the signal influences the distribution of power P over the harmonics and also in the power measurements P_i'. Thus, D and D_0 will be greater in a square signal than in a sinusoidal signal. The values of D and D_0 increase with the distortion of the input signal. The same applies to the D/P and D_0/P_0' ratios, which are always greater in square signals, compared to their sine-wave equivalents.
- Observe that the rest input powers calculated in square signals are smaller than those of their sinusoidal equivalents (at the same level, same frequency and same number of measured harmonics). This means that the distribution of input power in the higher order harmonics is greater in the harmonics closest to the fundamental, the greater the distortion. That is, in sinusoidal low distortion signals there may be a distribution of power in higher order harmonics important, but it is not in the closest to the fundamental, but in the farthest the lower the distortion. This explains relatively large power differences D in low distortion sinusoidal signals.

Table 6: Processing and summary results of experiment 2.

Results Summary (3dBm) Experiment2									
Sine Signal					***Squared Signal***				
f_0/THD	D(μw)	D_0(μw)	D/P %	D_0/P_0' %	f_0/THD	D(μw)	D_0(μw)	D/P %	D_0/P_0' %
50KHz/0.24%	537.68	53.78	26.75	3.65	50KHz/43.93%	602.13	235.75	29.96	19.98
100KHz/0.24%	513.75	51.38	25.56	3.43	100KHz/43.26%	577.28	233.73	28.72	19.49
1MHz/0.16%	534.23	53.43	26.58	3.62	1MHz/42.71%	591.50	228.71	29.43	19.07
10MHz/0.21%	581.10	58.11	28.91	4.07	10MHz/21.73%	810.37	128.78	40.32	11.24

VII. Conclusion

The extended relativity theoretical basis is the quantization hypothesis of the propagation velocity of any interaction with information in quantization intervals of size c in a vacuum.

This situation allows generalizing Einstein's relativity principle considering that "*the laws of nature are the same in any inertial reference system, regardless of its application speed coordinate*". Its justification is achieved through the Lorentz transformations of generic m_degree, which lets quantization of propagation velocities in electromagnetic interactions. Why? Because the Lorentz transformations of m_degree are a generalization of the Lorentz transformations, which admit observers and physical entities observed in any coordinate of generic speed, distinguishing between one and the other.

The Lorentz transformations of m_degree represent a formal justification of the speed of light quantization hypothesis, supported by the wave equation study, where implicitly arises the wave propagation speed that, traditionally, in any circumstance in a vacuum is c. However, this detailed wave equation study concludes that "*the wave propagation speed measured in a given observation does not depend on the origin of the wave, but precisely on the speed coordinate from which the measurement is made*". Then, a light wave originating in the speed m_coordinate, propagating with $(m+1)c$ velocity, will be seen thus if the observer moves within its same speed m_coordinate; in any other case, the observer detects the light with propagation velocity associated to its movement coordinate, for example, if the observer is in the speed 0_coordinate, the wave is seen with propagation velocity c.

The experimental support for the light velocity quantization hypothesis developed is based on the spectral study of harmonics in electromagnetic signals. The proposed experiments offer power discrepancies between the signals generated and those measured by spectral analysis. These differences, not explained by conventional theories, are explained by the quantization hypothesis of the propagation velocities in the different harmonics that compose these electromagnetic signals.

Two types of waves, sinusoidal and square, have been used and, as expected, it is concluded that for the same frequency and same effective value, the greater the distortion of the signal, the greater the power difference between the generated signal and the spectrally measured signal. This is due to the fact that the more power is distributed in the higher order harmonics, with respect to the fundamental harmonic which decreases its level, the greater the total power difference measured with respect to the generated, taking into account that,

1. Higher-order harmonics propagate at higher speed coordinates, that is, above the speed 0_coordinate.
2. The measurement is made from the speed 0_coordinate and in the power difference, the value of the fundamental harmonic does not intervene, nor of the first higher harmonic (65).
3. From the speed 0_coordinate, the signal propagation effect in other higher coordinates is observed, apparently with less power, except in the fundamental harmonic where the measure P_0' is higher than the expected value P_0, compatible with the quantization theory of the speed of light.

The distribution of input power in the higher order harmonics is greater in the harmonics closest to the fundamental one, the greater the distortion, as occurs with square signals. Thus, in low distortion signals we can find with a distribution of power in higher order harmonics important, power as much further from the fundamental harmonic as the lower the distortion. The relatively large power differences *D* obtained in low distortion signals are, therefore, another argument in favor of the quantization theory of the speed of light.

In addition, for the same type of signal, with the same shape, the higher the frequency *f*, the greater the power difference between generated and measured, due to the influence of the *K* parameter, function of f^2.

Appendix

The equipments used in the experiments for generating and measuring signals, with their technical specifications, are indicated below.

1. RF Synthesizer Hameg HM8134 [18]:

Range 1Hz to 1024MHz, Resolution 1Hz, spectral harmonic purity 1Hz to 1024MHz<-30dBc, output level accuracy ±0.5dBm, impedance 50Ω, VSWR<1,5

2. Spectrum Analyzer Rigol DSA815TG [19]:

Range 9KHz to 1.5GHz (-3dB), frequency resolution 1Hz, reference frequency 10MHz, RBW 10Hz to 1MHz, VBW 1Hz to 3MHz, SSB phase noise <-80dBc/Hz (10KHz), amplitude range DANL to +20dBm, preamplifier with gain 20dB, zero span, markers, input impedance 50Ω (selectable 75 Ω), attenuator 0 to 30dB, tracking generator 100KHz to 1.5GHz (-20dBm to 0dBm).

3. Digital Oscilloscope Tektronix TDS220 [20]:

Sample range 1GS/s, Frequency band width 100MHz, input impedance 1MΩ, 20pF, two channel dual, maximum input 300Vrms.

4. Function/arbitrary waveform generator AD Instruments AD8610 [21]:

Bandwidth and max output frequency 10MHz, frequency resolution 1μHz, sample rate 125MS/s, 2 output channels, waveform sine, square, triangular, pulse, Gaussian, noise, arbitrary, modulation in AM, FM, PM, FSK, ASK, PWM, burst, amplitude range 2mVpp to 10Vpp (50Ω).

For experiment1, equipments 1, 2 and 3 were used. For experiment2, equipments 2, 3 and 4 were used. To solve the different systems of linear equations proposed in each of experiments 1 and 2, the Gauss-Jordan method was used, applied in a practical way through [25]. The images corresponding to the development of experiment1 and experiment2 can be obtained in [26].

References

[1]. A. Einstein, A., Zur Elektrodynamik bewegter Körper, *Annalen der Physik, 17 (10),* 1905, 891–921, doi:10.1002/andp.19053221004. English translation.

[2]. B.G. Levich, *Física Teórica 1: Teoría del campo electromagnetico y teoría de la relatividad* (Editorial Reverté S.A.: Barcelona, 1974).

[3]. O. Darrigol, The Genesis of the theory of relativity, *Séminaire Poincaré, 1,* 2005,1–22, doi:10.1007/3-7643-7436-5_1.

[4]. P. Pascual and J. I. Latorre, La teoría de la relatividad especial, *Revista Española de Física*, *19 (1)*, 2005, 4-9.

[5]. M.J. Feigenbaum, The theory of relativity-Galileo's child, *Arxiv: physics.class-ph/0806.1234v1*, 2008.

[6]. L.J. Boya and M. Santander, Paradojas relativistas, *Revista Española de Física*, *19 (4)*, 2005,17-24.

[7]. J. Joglar Alcubilla, Extended relativity theory, *General Science Journal*, June 2017.

[8]. H. Poincaré , The theory of Lorentz and the principle of reaction, *Archives neerlandaises des Sciences exactes et naturelles, series 2, 5*, 1900, 252-278

[9]. A. Galiautdinov, Derivation of the Lorentz transformation without the use of Einstein's second postulate, *Arxiv: physics.class-ph/1701.00270v1*, 2017.

[10]. R. Heras, A review of Voig's transformations in the framework of special relativity, *Arxiv: physics.hist-ph/1411.2559v4*, 2017.

[11]. UP Commons, *Análisis espectral basado en FFT*, 6, (Universitat Politécnica de Catalunya, https://upcommons.upc.edu/bitstream/handle/2099.1/9988/09_analisis_FFT.pdf?sequence=9&isAllowed=y , 2009), 57-74.

[12]. J. Martín Montalban, Analizadores de espectros: medidas de distorsión, Denver Metrología Electrónica S.L., https://www.denver.es/wp-content/uploads/2015/08/Analizadores-de-Espectros-Medidas-de-Distorsi%C3%B3n.pdf (online), 2015

[13]. J, Bernal, P.Gómez y J. Bobadilla, Una visión práctica en el uso de la transformada de Fourier como herramienta para el análisis espectral de la voz, Universidad politécnica de Madrid, http://stel.ub.edu/labfon/sites/default/files/EFE-X-JBernal_PGomez_JBobadilla-FFT_una_vision_practica_herramienta_para_el_analisis_espectral_de_la_voz.pdf (online), 1999

[14]. N.L. Zakamska, Theory of Special Relativity, *Arxiv: physics.ed-ph/1511.02121v3*, 2017

[15]. A. Aparicio, *Armónicos en las redes eléctricas*, 2, (Universidad Politécnica Salesiana, https://www.google.es/url?sa=t&rct=j&q=&esrc=s&source=web&cd=13&cad=rja&uact=8&ved=0ahUKEwjZxsbB84TbAhVII8AKHSVdDz8QFgheMAw&url=https%3A%2F%2Fes.scribd.com%2Fdocument%2F275810327%2FArmonicos&usg=AOvVaw0VvDAYFIn67uXJ9LVbt3Yi , 2008), 23-55.

[16]. Eisberg R. and Resnick R, Fotones-Propiedades corpusculares de la Radiación, in Noriega (Ed.), *Física Cuántica*, 2 (Mexico:Limusa, 1989), 45-75, ISBN 9681804198

[17]. J.L. Varela Villanueva y F.J. Alvarado Ramirez, *Banco de pruebas para filtrado de armónicos en las redes eléctricas*, Tesis, Universidad Politécnica Salesiana, Ecuador, 2015

[18]. Hameg GmbH, *Manual RF synthesizer HM8134* (Germany: Hameg Instruments, 1998).

[19]. Rigol, *Rigol User's Guide DSA800 Series Spectrum Analyzer* (China: Rigol Technologies Inc., 2014).

[20]. Tektronix, *Digital Oscilloscope TDS220, User Manual* (EEUU: Tektronix Inc., 1995).

[21]. AD Instruments, *Function/arbitrary waveform generator AD8610 User Manual* (Australia: AD Instruments Inc., 2014).

[22]. *El analizador de distorsión (analógico)*, 9, http://users.salleurl.edu/~se04066/mesures/p09.pdf (online)

[23]. D. Shmilovitz, On the definition of total harmonic distortion and its effect on measurement interpretation, *IEEE Transactions on Power Delivery*, 20(1), 2006, 526-528.
[24]. G.E. Mog and E. Parente Ribeiro, Total harmonic distortion calculation by filtering for power quality monitoring, *Transmission and Distribution Conference and Exposition: LatinAmerica 2004 IEEE/PES*, DOI 10.1109/TDC.2004.1432452
[25]. Matrix Calculator, *Solución de Sistemas de Ecuaciones Lineales*, https://matrixcalc.org/es/slu.html
[26]. J. Joglar Alcubilla, Light Velocity Quantization and Harmonic Spectral Analysis, Dropbox, 2018, https://www.dropbox.com/sh/ulmlds0ceddtkl3/AAB52LRYtKOr3xu7xbxZlgssa?dl=0

Javier Joglar Alcubilla, " Light Velocity Quantization and Harmonic Spectral Analysis. "IOSR Journal of Applied Physics (IOSR-JAP) , vol. 10, no. 4, 2018, pp. 57-71.